Electrical and photoelectrical studies of plasma polymerized acrylonitrile

SUJATA B DAKE and S V BHORASKAR
Department of Physics, University of Poona, Pune 411 007, India

Abstract. The electrical and photoelectrical properties of plasma polymerized acrylonitrile (PAN) are reported. The polymer films were studied in silver-PAN-silver systems. Electrical conductivity at room temperature was of the order of 10^{-11} ohm^{-1} cm^{-1}. The space charge limited current (SCLC) studies at room temperature and thermally stimulated current studies (TSC) over a temperature range of 290–500°K led to a clear understanding of carrier concentration, carrier mobility, trapping levels and activation energies. Photoelectric measurements were used to draw a band picture in plasma deposited PAN.

Keywords. Plasma polymerization; polyacrylonitrile; thermally stimulated current; SCLC.

PACS No. 73·60

1. Introduction

Recently there has been a great deal of interest in semiconducting organic polymers as electronic materials in various applications proposed by Metz *et al* (1982), Lautfy and Haiao (1982), Mort and Pfister (1982). It is well known that polyacrylonitrile can be made semiconductive by pyrolysis (heat treatment in inert atmosphere) and conductivity can be controlled to a desired level. This kind of conducting organic polymers on substrates is useful in micro-electronics and several electron devices including solar cells and plastic batteries. Considering the increased applications of thin films of PAN in devices in recent years, we undertook an extensive investigation of the electrical properties of plasma polymerized thin films. In spite of the available literature on the electrical measurements in pyrolised PAN (Suzuki *et al* 1975; Hirai and Nakada 1968) a clear picture of the energy band is not available for plasma polymerized PAN. This paper reports the application of space charge limited conduction, photoconduction and optical absorption measurements for determining the band picture parameter in plasma polymerized PAN. Thermally stimulated current measurements led to the determination of dominant trapping levels.

2. Experimental

2.1 *Preparation of the film*

Thin films of PAN were deposited on cleaned glass substrates using plasma polymerization technique. Substrates were placed between two parallel stainless steel circular

electrodes, in a vacuum chamber which was initially evacuated to a pressure of 10^{-6} torr by mercury diffusion pump with three liquid nitrogen traps to avoid any contamination. A fine needle valve was used for maintaining the monomer pressure at 10^{-1} torr. Consequently, alternating voltage was applied to the condenser plates for establishing stable glow discharge in the chamber. The rate of polymer deposition was studied at three different frequencies *viz* 50 Hz, 4 MHz and 10 MHz as shown in figure 1. The frequency of electric field was optimized at 10 MHz due to fast deposition rate, uniformity of the films and better sticking coefficient of PAN on glass substrates at this frequency.

Thickness of the film was determined by gravimetric analysis and optical method. For optical measurements, the film was partly deposited on the substrate forming a sharp edge and then coated with silver.

$1\cdot2$ μm thick films were used for further experimentation.

2.2 *Electric and photoelectric measurements*

Electrical conductivity was measured on sandwich-type specimens. Vacuum evaporated silver electrodes were used as contacts. Current was detected under equilibrium conditions of temperature and electric field, using electrometer amplifier. For photoconductivity measurements, sandwiched specimens were irradiated with white light of a tungsten lamp (60 W). SnO_2 was used as a transparent electrode, the other was a silver electrode. Filters of 200 nm bandwidth were used to measure spectral sensitivity of the photocurrent.

Thermally stimulated current was measured by heating the specimen at a rate of $0.2°K$ sec^{-1}. Current was recorded over an X–Y recorder.

3. Results and discussion

Plasma polymerized films of acrylonitrile, obtained on glass substrates were pale yellowish having a smooth surface. The colour of the film changed from yellowish to brown with increasing thickness.

Figure 1 shows the variation of the film thickness with time of deposition at various applied electrical frequencies. The film thickness increases smoothly for about 20–25 min in almost all the cases and then increases at a higher rate. The process of plasma polymerization takes place through the formation of free radicals and charged species. The increasing concentration of free radicals in the plasma increased the deposition rate. The other important parameter was the system equilibrium which was dependent on the dynamic vacuum conditions, monomer feeding rate and the rate of free radical formation in the plasma. The observed results show that the system equilibrium could be achieved after 20–25 min in the present system. Further increase in free radicals increases the deposition rate. This was also visibly observed by the change in the intensity of colour of the plasma.

3.1 *SCLC measurements*

The current for the sandwiched structure of Ag-PAN-Ag was recorded in thermal equilibrium. From these measurements, I-V characteristics were obtained at different temperatures ranging from 20–140°C. The mechanism of electrical conduction in thin
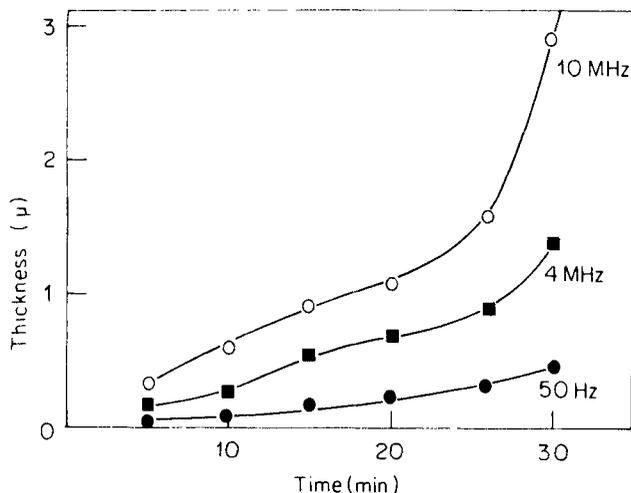
Figure 1. Variation of film thickness polymerized at 10 MHz, 4 MHz and 50 Hz as a function of time.

insulating films using few important theoretical models formulated by Lamb (1967) is applied to analyse the I–V characteristics. According to the basic assumptions, if an ohmic contact is made at the surface of an insulator, electrons flow from the metal to the conduction band of the insulator. Due to injected charges, there is a generation of space charge near the electrodes which affect the conduction mechanism. As an effect, ohmic conduction (linear I–V characteristic) changes into space charge limited (scl) (I–V^2 characteristic) conduction in the presence of traps, as the applied electric field is increased. The current in the two regions are given by,

and

$$I_{ohmic} = n \mu e V / s,$$ (1)

$$I_{SCL} = \frac{9}{8} \mu \varepsilon V^2 \theta \frac{1}{s^3},$$ (2)

where n is the charge carrier concentration at thermal equilibrium, μ the microscopic mobility, V the voltage across the sample, ε the dielectric constant, s the sample thickness and θ the ratio of free to trapped charge carriers.

The I–V plots in figures 2 and 3 indicate that the conduction at room temperature follows sclc characteristics while for elevated temperatures, it is ohmic for all field strengths.

At first sight, the room temperature behaviour may be analysed. Figure 2 indicates that this I–V plot consists of an ohmic region with a slope approximately unity for voltages up to a value indicated by V_{tr2}. Above this, the behaviour is quadratic in nature up to a value denoted by V_{TFL} in excess of which, the current increases sharply to a trap free sclc. V_{tr1} is the voltage at which I_{ohmic} changes into I_{SCL} in the absence of traps and is obtained by (1) and (2) corresponding to trap free sclc.

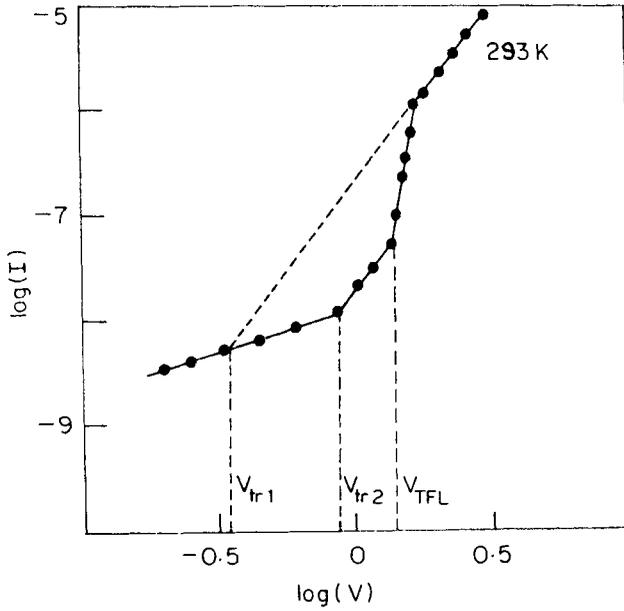$$V_{tr1} = \frac{8}{9} \frac{ns^2 e}{\varepsilon}.$$ (3)

Figure 2. Logarithmic plot of current voltage at 293°K, exhibits one carrier space-charge limited conduction; characteristic $V_{tr1} = 350$ mV and $V_{tr2} = 870$ mV. Regions are (i) Ohmic (ii) SCLC in presence of traps (iii) transition from SCLC with traps to SCLC without traps and (iv) SCLC in absence of traps.
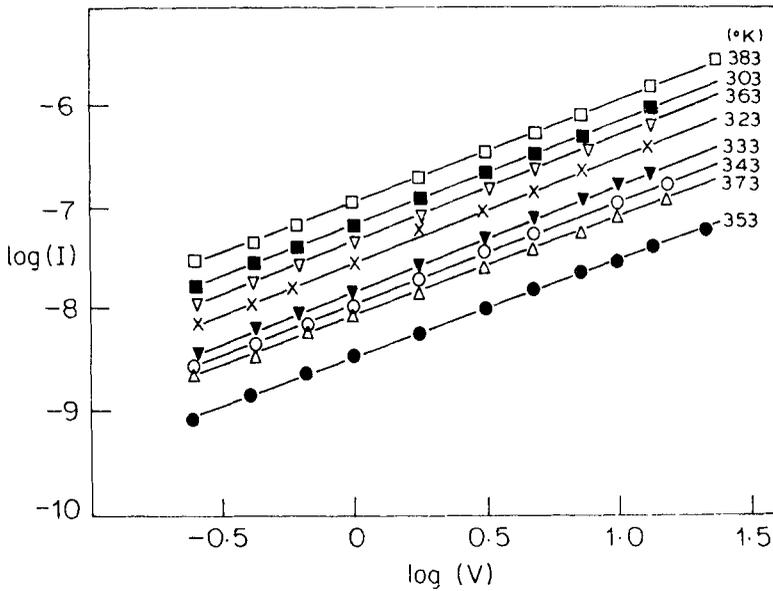

Figure 3. Logarithmic plots of current and voltage characteristics at elevated temperatures, showing ohmic nature.

Further extending the theory of SCLC given by Lamb (1967) one obtains the transition voltage at which the conduction changes from ohmic to SCLC behaviour in the presence of traps as,

$$V_{tr2} = \frac{8}{9} \frac{ns^2 e}{\varepsilon \theta}. \tag{4}$$

Voltages V_{tr1} and V_{tr2} in the present experiments are 350 and 870 mV respectively. Using the dielectric constant for PAN the carrier concentration at room temperature was calculated from (3) as equal to 9×10^{12} cm^{-3}, at a field strength of 3×10^3 V cm^{-1}. Mobility was then determined to be $1 \cdot 1 \times 10^{-7}$ cm^2 V^{-1} sec^{-1} from the ohmic current in (1).

The density of trapped charges was also calculated using the transition voltage from space charge limited to trap filled region, V_{TFL}, given by

$$V_{TFL} = \frac{N_t s^2 e}{\varepsilon}. \tag{5}$$

The density of trapped charges was equal to $2 \cdot 96 \times 10^{13}$ cm^{-3}. At higher temperatures (figure 3) disappearence of the SCLC region, may perhaps be explained as due to increase in the carrier concentration n, with increase in temperature. Now, as transition from ohmic to SCLC is obtained at a voltage where concentration of the injected charges become equal to the intrinsic concentration in thermal equilibrium, this transition will occur at a sufficiently high voltage. If the required voltage falls beyond the breakdown limit of the film, then the transition may not be observed. We expect this to occur in our samples which have shown the ohmic character over the observed range of voltages before breakdown occurred at around 80 V at room temperature.

The irregular variation of I–V plots with temperature is the result of detrapping phenomenon as will be explained in § 3.2.

The temperature dependence of the intrinsic concentration in thermal equilibrium is given by

$$n = n_0 \exp(-E_g/2kT).$$

Samples were annealed at 150°C till the TSC peaks smoothened out (figures 4 and 5). From this current thermogram a plot of $\ln I$ vs $1/T$ was obtained. The slope of the straight line gave the value of half the band gap. This was determined to be $0 \cdot 715$ eV and thus the band gap for PAN was determined to be $1 \cdot 43$ eV. This value agrees with the band gap calculated by photoconductivity measurement (described in § 3.3) which shows that the material is an intrinsic semiconductor. The mechanism of conduction in intrinsic PAN is, therefore, seen to be mainly band conduction as the temperature dependence of conduction gives an activation energy related to band transition.

3.2 TSC measurements

If one looks into the variation of current with temperature, it shows dips and peaks at different temperatures (figure 4). This is the reason why in figure 2, the I–V plots do not exhibit any regular trend with temperature. The origin of short circuited current in M–I–M structure is described elsewhere. Several processes contribute to the thermally stimulated current in insulators. Immobilized and thermally released space charges produce TSC in insulators. In polar insulators, the disorder of the dipoles may also
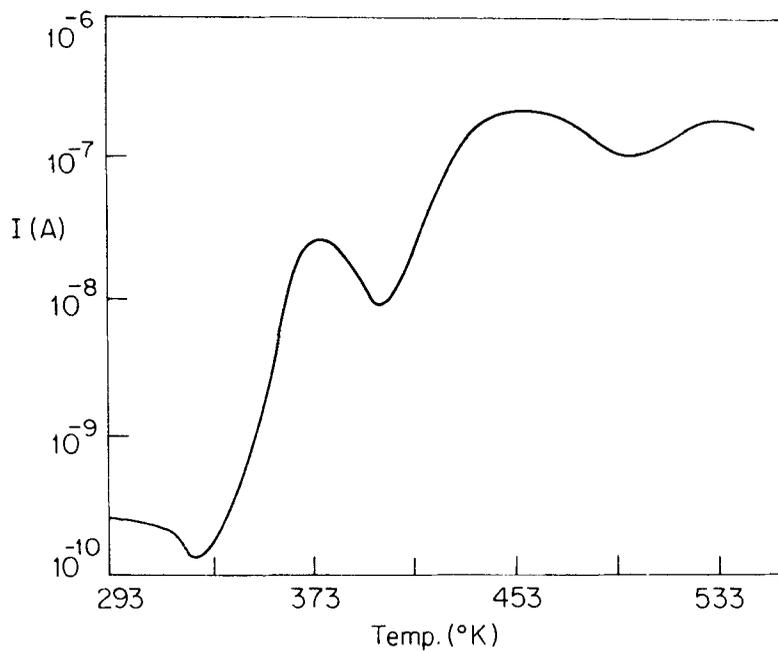
Sujata B Dake and S V Bhoraskar

Figure 4. TSC spectrum of PAN under zero bias condition, peaks obtained at 331 K, 375 K and 453 K.
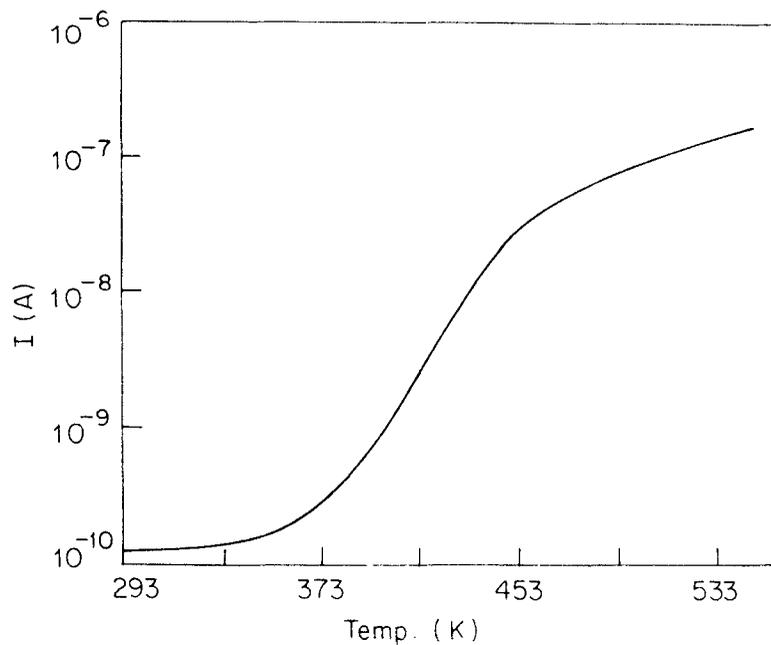

Figure 5. TSC spectrum of annealed sample of PAN.

contribute to the TSC. The plasma polymerized film of PAN has every chance, of accumulating space changes during the film formation. Moreover, the film showed the presence of a very small intrinsic voltage (of the order of few mV) possibly, due to the preferential orientation of nitrile polar groups—CN during formation of the film. When the specimen is short circuited, charge migration and disorientation of dipoles develop a current in the external circuit. As the charges move in the system, they may either get trapped again or recombine with the opposite charges. As mobility and relaxation time change exponentially with temperature, the thermally stimulated short circuit current increases exponentially. The detrapped charge carriers constitute peaks activated from their depths below the conduction band. The low temperature tail of each peak follows an Arrhenius relation and, therefore, plots of $\log I$ vs $1/T$ are straight lines with slopes related to the activation energies.

Peaks were observed at around 58, 103 and 180°C as shown in figure 4. The peaks at 103 and 180°C may be associated with randomization of nitrile side groups and microscopic charge displacements respectively as assigned by Stupp and Carr (1975) for their TSC peaks at 100 and 190°C. Transition around 100°C was named as beta peak by Suematsu *et al* (1983) and the same is named as γ peak by Stupp and Carr (1975).

The thermogram in figure 4 shows the first peak occurring at 58°C which is in opposite direction to the peaks obtained at 103 and 180°C. As already mentioned, the film of PAN in Ag-PAN-Ag structure showed a small amount of intrinsic voltage as its inherent property, which must be due to dipole orientation of polar nitrile groups during the polymerization. As the temperature is slowly increased above room temperature the thermally generated carriers move along the intrinsic field. This in effect will reduce the built-in voltage and will slowly build a space charge in the opposite direction. This may be the reason why the peaks at 58°C and those at 103 and 180°C are opposite in sense. Reversal in polarity in the TSC peaks is also revealed in the results of Stupp and Carr (1975). However, the origin of these peaks may be associated with the history of the samples.

The activation energies associated with the detrapping process, as a consequence of which TSC peaks are observed, were calculated by the low temperature tails of the peaks. The trap levels are indicated in figure 8, on the energy band diagram.

3.3 *Photoelectric effect*

Photoconductivity was measured by plotting ohmic I–V characteristics in the presence of light. The maximum photoconductive quantum efficiency was determined to be 10^{-5} carriers per photon at an incident energy of 2·5 eV. The spectral response of photoconductivity is plotted in figure 6. The optical absorption of PAN is also shown in the same figure. A close correspondence is observed between the nature of photocurrent and optical absorption. From the data of optical absorption, the absorption coefficient k was determined. A plot of $k^{1/2}$ against $h\nu$ (figure 7) was a straight-line and gave an intercept on the $h\nu$ axis at 1·34 eV. This corresponds to the bandgap of the specimen. The value of optical absorption coefficient in this material is determined to be $1·6 \times 10^4$ cm^{-1} at 2·17 eV. An absorption coefficient less than 10^5 cm^{-1} may correspond to indirect bandgap semiconductors because direct band gap semiconductors are reported to have an optical absorption coefficient equal to or larger than 10^3 cm^{-1} (Dixon and Leslie 1978; Brennan *et al* 1962). Moreover a slow variation of optical absorption coefficient with $h\nu$ also indicate that the specimen is an indirect band gap
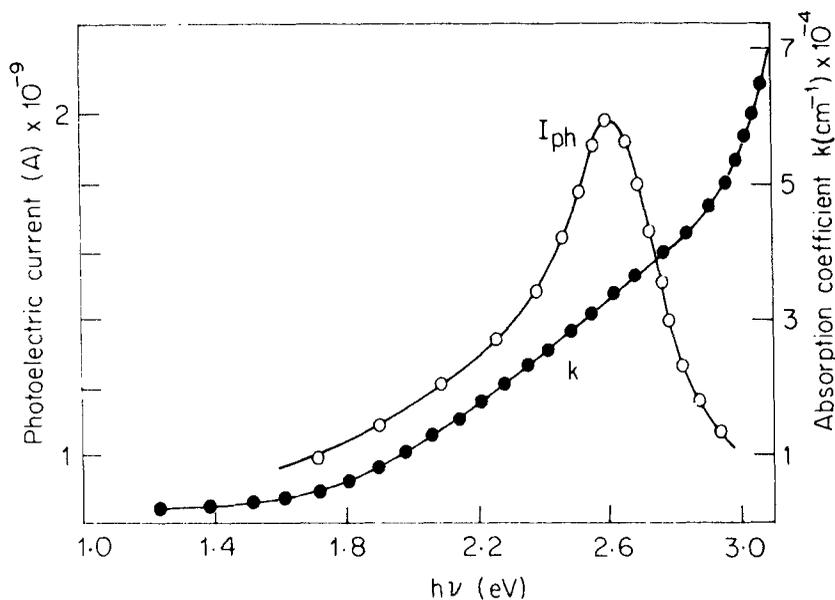
Figure 6. Spectral response to photocurrent I_{ph} and absorption coefficient k.
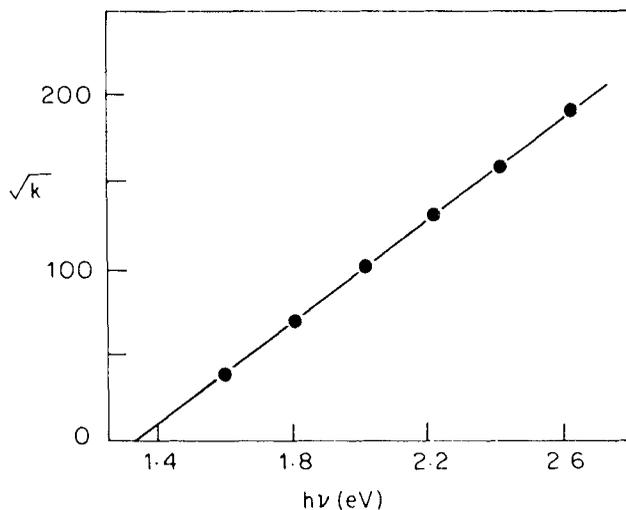

Figure 7. Plots of square root of absorption coefficient as a function of energy. Band gap was determined by extrapolating the straight line to the energy axis.

semiconductor. A relation between $(hv-Eg)^2$ with optical absorption k shows a straight-line (figure 7) proving that the transition is indirect.

The bandgap calculated from these observations is suitable for absorption in the visible range and also the value of the absorption coefficient thus makes the material suitable for photovoltaic devices. This was proposed by Metz *et al* (1982) and the present results supports its validity. A possible band picture is shown in figure 8 for PAN.
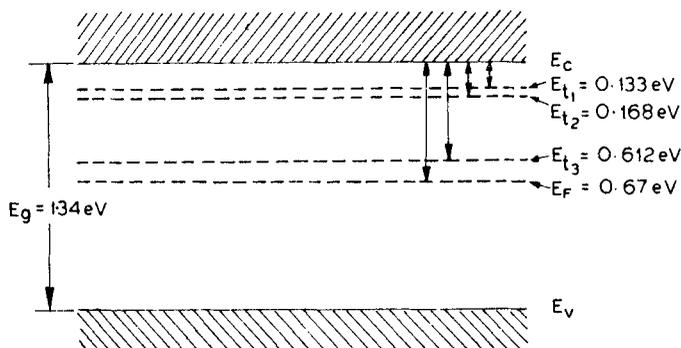
Figure 8. Possible energy band model for PAN.

Assuming an intrinsic nature in polyacrylonitrile as reported by Tadaki and Osamu (1968) and Brennan *et al* (1962), the Fermi level is shown in the middle of the bandgap. Our results of TSC and optical measurements strongly support the band conduction.

4. Conclusion

From the experimental results, it can be concluded that polyacrylonitrile can be deposited by plasma polymerization technique to a desired thickness which can suit the requirements in electron devices, by suitably controlling the electrical conduction to a desired level. Moreover its photoelectrical properties in the visible range make this material useful for photovoltaic devices. The sample is proved to be an intrinsic semiconductor and so, doping with donors and acceptor impurities, can be more useful for devices.

Acknowledgements

References

Brennan W D, Brophy J J and Schonhorn H 1962 *Organic semiconductors* (eds) J J Brophy and J W Buttrey (New York: The Macmillan) 159
Dixon A E and Leslie J D (eds) 1973 *Solar energy conversion: An introductory course* (Canada: Pergamon Press)
Hirai T and Nakada O 1968 *Jpn J. Appl. Phys.* **7** 112
Lacombe E M 1957 *J. Polym. Sci.* **24** 152
Lamb D R 1967 *Electrical conduction mechanism in thin insulating films* (London: Methuen)
Loutfy P O and Haiao C K 1982 *Polym. Prepr.* **23** 237
Metz P D, Tech H and Welhelm W J 1982 *Polym. Prepr.* **23** 239
Mort J and Pfister G (eds) 1982 *Electronic properties of polymers* (New York: John Wiley)
Stupp S I and Carr S H 1975 *J. Appl. Phys.* **46** 4120
Suematsu K, Nakamura K and Takada J 1983 *Polym. J.* **15** 71
Suzuki M, Takahashi K and Mitani S 1975 *Jpn J. Appl. Phys.* **14** 741